J. Cent. South Univ. (2022) 29: 1289−1304
DOI: https://doi.org/10.1007/s11771-022-4989-6

Springer

Extending application of asymmetric semi-circular bend specimen to investigate mixed mode I/II fracture behavior of granite

WU Qiu-hong(吴秋红)[1], XIE Cheng-long(谢成龙)[1], XIE You-sheng(谢柚生)[2]*,
ZHAO Yan-lin(赵延林)[1], LI Xue-feng(李学锋)[3], LIU Jie(刘杰)[4], WENG Lei(翁磊)[5]

1. Work Safety Key Lab on Prevention and Control of Gas and Roof Disasters for Southern Coal Mines, Hunan Provincial Key Laboratory of Safe Mining Techniques of Coal Mines, Hunan University of Science and Technology, Xiangtan 411201, China;
2. School of Resources and Safety Engineering, Central South University, Changsha 410083, China;
3. College of Resources and Metallurgy, Guangxi University, Nanning 530004, China;
4. Department of Building Engineering, Hunan Institute of Engineering, Xiangtan 411101, China;
5. School of Civil Engineering, Wuhan University, Wuhan 430072, China

Abstract: The asymmetric semi-circular bend (ASCB) specimen has been proposed to investigate the cracking behavior in different geo and construction materials and attracted the attention of researchers due to its advantages. However, there are few studies on the fracture toughness determination of rock materials. In this work, a series of fracture tests were performed with the ASCB specimens made of granite. The onset of fracture, crack initiation angle and crack propagating trajectory was analyzed in detail combined with several mixed mode fracture criteria. The influence of the crack length on the mode I/II fracture toughness was studied. A comparison between the fracture toughness ratios predicted by varying criteria and experimental results was conducted. The relationship between experimentally determined crack initiation angles and curves of the generalized maximum tangential stress (GMTS) criterion was obtained. The fracture process of the specimen was recorded with the high-speed camera. The shortcomings of the ASCB specimens for the fracture toughness determination of rock materials were discussed. The results may provide a reference for analysis of mixed mode I and II fracture behavior of brittle materials.

Key words: asymmetric semi-circular bend specimen; rock fracture toughness; crack growth trajectory; crack initiation angle; semi-circular bending; generalized maximum tangential stress criterion

Cite this article as: WU Qiu-hong, XIE Cheng-long, XIE You-sheng, ZHAO Yan-lin, LI Xue-feng, LIU Jie, WENG Lei. Extending application of asymmetric semi-circular bend specimen to investigate mixed mode I/II fracture behavior of granite [J]. Journal of Central South University, 2022, 29(4): 1289−1304. DOI: https://doi.org/10.1007/s11771-022-4989-6.

1 Introduction

Rock mass, an important characteristic of which is the inevitable existence of cracks and flaws, is applied in various engineering constructions [1]. These defects acting as stress raisers increase the concentration of stress in the vicinity of their tips and decrease significantly the load bearing capacity of rock mass, possibly

Foundation item: Projects(52004182, 51804110, 51904101) supported by the National Natural Science Foundation of China; Project (2020JJ5188) supported by the Natural Science Foundation of Hunan Province, China
Received date: 2021-03-16; **Accepted date:** 2021-06-19
Corresponding author: XIE You-sheng, PhD; Tel: +86-17399665744; E-mail: yousheng_xie@163.com; ORCID: https://orcid.org/0000-0001-6023-6347

resulting in catastrophic brittle failures. Fortunately, a commonly used fracture parameter called fracture toughness has been proposed to describe the critical states of stresses or energy in the vicinity of the crack tip and to study crack initiation and propagation. This parameter is usually used in the discussions of foundations, natural and man-made slopes, surface and underground excavations, tunneling, mining, etc [2]. Accordingly, the determination of fracture toughness for rocks has become an indispensable part for the design, construction and stability evaluation of rock engineering.

Fracture in rock mass usually happens in a complicated strain or stress environment, due to its varying sizes, orientations and locations [3]. There are three basic deformation modes for a cracked body according to its applied stress conditions: mode I (opening mode), mode II (sliding mode) and mode III (tearing mode). Of the three modes, the mode I fracture is the simplest and the most common failure mode of rock material due to brittle fracture [4]. Therefore, previous researchers have already developed several testing techniques and specimen configurations to investigate mode I fracture toughness. Short rod specimen [5], chevron bend specimen [5] and straight edge cracked round bar bend specimen [6] are three cylindrical specimens. Since they are easily manufactured from rock cores, semi-circular and disc shaped specimens in rock fracture resistance tests are generally preferred compared with the three specimens above. Semi-circular bending (SCB) specimen [7, 8] and chevron notched semi-circular bending specimen [9] are two commonly used semi-circular specimens, while cracked straight through Brazilian disk specimen [10], flattened Brazilian disk specimen [11, 12], cracked chevron notched Brazilian disc specimen [13], holed-flattened Brazilian disc method specimen [14], edge notched disc bend specimen [15], edge cracked disc specimen [16, 17] and holed-cracked flattened Brazilian disc specimen [18] are typical Brazilian type specimens.

In general, rock materials under low or no confining pressure conditions exhibit clear brittle behavior and are prone to failure caused by tensile stress [19−21]. Therefore, it is understandable that most of the previous studies on rock fracture mechanics had focused on mode I crack propagation. However, cracks and flaws in rock mass are more likely to be subjected to various mixed-mode (i.e. combinations of mode I and mode II) loading rather than pure mode I loading. Mixed mode fracture toughness determination of rocks can also be achieved by using some of the above-mentioned specimens [22−24].

Although some of these specimens are now accepted as the methods suggested by the International Society for Rock Mechanics (ISRM), there are still some disadvantages that cannot be ignored in practical application including direct tensile load application on rock specimens, complex preparations and cumbersome steps. Short rod specimen and SCB specimen are two good examples about this. Short rod specimen can ensure the crack development at the sharp tip during the early stage of test loading; however, the application of it requires cumbersome steps to be followed and thus needs more efforts to perform a test. A tensile load is directly applied perpendicular to the initial chevron notch plane, which may result in the premature failure of the contact bonding between the loading platen and specimen, especially for hard rocks with high tensile strength [25]. Also, the preparation of chevron-notched specimens with enough precision requires special care. For the SCB specimen, it has been widely used for fracture toughness determination of geomaterials owing to inherent favourable properties such as its simplicity, minimal requirement of machining and the convenience of testing. The different combinations of mode I and mode II are obtained by producing specimens with varying crack angles. Pure mode II loading condition may require that the SCB specimen contains an initial crack with an inclination angle of greater than 50° [26 − 28]. However, an unwanted fracture may occur in the process of preparing such SCB specimen [29].

A classic SCB specimen for the improved test configuration, namely ASCB specimen, was proposed in Ref. [30] in order to remove the above-mentioned limitations of the SCB specimen. Varying mode mixities in the ASCB specimen is obtained by changing the locations of two bottom supports (S_1 and S_2). The new specimen has the

same geometrical dimensions as the conventional one used for performing pure mode I fracture test, and thus it is easy to be manufactured. The new specimen attracts the attention of researchers in the field of rock fracture mechanics with its various advantages including simple geometry, inexpensive manufacturing process and easy test conducting procedure. Accordingly, the ASCB specimens are widely used to investigate mixed mode fracture behavior of different geo and construction materials, such as polymethylmethacrylate (PMMA) [30], foam [31], and asphalt concrete [32, 33]. ALIHA [34] conducted fracture toughness experiments to predict mode II fracture toughness of hot mix asphalt mixtures by using ASCB specimens. FAKHRI et al [35] studied crack behaviors of roller compacted concrete containing reclaimed asphalt pavement and crumb rubber. Previous studies under asymmetric three-point bend loading conditions are fundamental and have contributed to a better understanding of the fracture mechanism of materials. However, there are few studies to investigate the cracking behavior in rock material, especially the effect of the crack length on the fracture behavior of rock using the ASCB specimen [36, 37]. After all, there are more natural fractures and more significant heterogeneities within rock materials, and the initial crack size has a great influence on the fracture properties of rock. Therefore, it is necessary to investigate the mixed mode I and II fracture behavior of a rock with different crack lengths using ASCB specimen.

The aim of this work is to extend the application of the ASCB specimen for fracture resistance determination of rock materials, in the hope of providing a better understanding of its application. To this end, we performed a series of fracture tests by using the ASCB specimens made of granite. The onset of fracture, crack initiation angle and crack propagating trajectory was discussed in detail combined with several mixed mode fracture criteria.

2 Material and experimental method

2.1 Material

A white granite collected from the north of China was chosen for conducting mixed mode fracture tests on rock materials using the ASCB geometry. The basic mechanical properties of the tested samples included elastic modulus of 87.2 GPa, Poisson ratio of 0.23, mean tensile strength of 11.73 MPa and uniaxial compressive strength of 223 MPa. For preparing test specimens, disc specimens with a diameter of 94 mm were firstly drilled from a sheet of granite plate of approximately 26 mm in thickness. A disc specimen obtained was then sliced into two equal semi-circular specimens by using a saw blade of 2.5 mm in thickness. A notch with the required depth was generated along the center line of the semi-circular specimen by using a saw blade of 1.8 mm in thickness. The manufactured specimen is shown in Figure 1(a). To explore the influence of the ratio of crack length a to radius R, three values of the ratio were considered: a/R=0.3, 0.4 and 0.5.

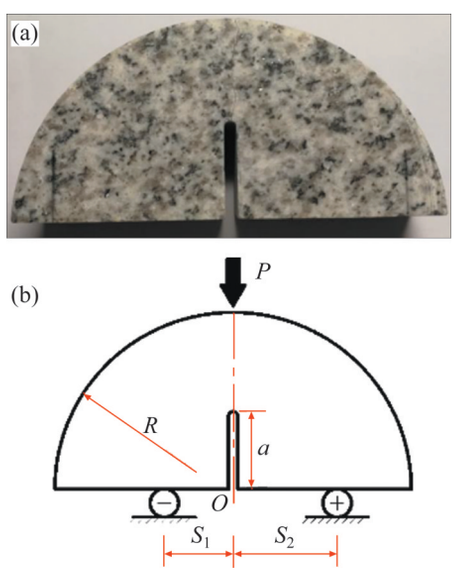

Figure 1 ASCB specimen for fracture toughness determination: (a) Manufactured specimen; (b) Specimen subjected to asymmetric three-point bend loading

2.2 Experimental method

The fracture tests were performed in a servo controlled testing machine. The load was measured with a 20 kN load cell with ±0.5% error at full scale. The deformation was measured by an inductive extensometer with ±0.1% error at full scale and automatic calibration. The force–displacement curves and fracture loads were recorded automatically during testing.

The specimen was located on two bottom supports and compressed by the vertical load P. As shown in Figure 1(b), S_1 (non-fixed support) and S_2

(fixed support) are shorter and longer distances between the supports and crack, respectively. During testing, a monotonic compressive load was applied on the specimen under displacement control condition at a displacement rate of 0.12 mm/min. In order to investigate the fracture behavior, a high speed (HS) camera system [20, 38] was used to photograph the ASCB specimen during testing. The system consists of a complementary metal oxide semiconductor (CMOS) sensor-based HS camera (Photron FASTCAM SA1.1, San Diego, California), a macro lens, a set of extension tubes, and a ring-shaped flashlight. The resolution of the image is 448×224 pixels at a frame rate of 50000 frame/s.

As shown in Figure 1(b), the distance S_2 was set equal to 37.6 mm for all the experiments. Three groups of S_1 were chosen for experiments, including S_1=37.6 mm, 25.0 mm, 15.0 mm, 9.7 mm (mixed mode I=II) and 5.3 mm (pure mode II) for a/R=0.3, S_1=37.6 mm, 25.0 mm, 15.0 mm, 8.8 mm (mixed mode I=II) and 4.1 mm (pure mode II) for a/R=0.4 and S_1=37.6 mm, 25.0 mm, 15.0 mm, 7.3 mm (mixed mode I=II) and 3.3 mm (pure mode II) for a/R=0.5. Furthermore, to examine the repeatability of the test results, three tests were performed for each loading mode, giving a total of 45 fracture tests.

3 Calculation of crack parameters

Prior to using the ASCB specimen, it is necessary to calculate several crack parameters like mode I and II geometry factors (Y_I and Y_{II}) and normalized T-stress (T*) for varying combinations of loading conditions and specimen geometries by using the finite element method. More details on the calculations will be elaborated in the subsequent section.

The stress intensity factors (SIF) (K_I and K_{II}) and T-stress (T) corresponding to the onset of fracture for the ASCB specimen can be written as [30]:

$$\begin{cases} K_I = Y_I\left(a/R, S_1/R, S_2/R\right)\dfrac{P_f}{2Rt}\sqrt{\pi a} \\ K_{II} = Y_{II}\left(a/R, S_1/R, S_2/R\right)\dfrac{P_f}{2Rt}\sqrt{\pi a} \\ T = T^*\left(a/R, S_1/R, S_2/R\right)\dfrac{P_f}{2Rt} \end{cases} \quad (1)$$

where Y_I and Y_{II} are the geometry factors of mode I and mode II, respectively; T* is the normalized T-stress; t is the specimen thickness; P_f is defined as the fracture load of the specimen and a/R denotes the crack length ratio. Varying finite element models for the ASCB specimen was built for the calculation of three crack parameters using ABAQUS software. In these models, the following parameters were applied: R=47 mm, P=1 kN, crack length ratios a/R= 0.3, 0.4 and 0.5, elastic modulus E=87.2 GPa, Poisson ratio v=0.23. Particular attention should be paid to the settings of S_1 and S_2. S_2 was set to a fixed value of 37.6 mm (i.e. S_2/R=0.8), while S1 varied from 37.6 mm to nearly zero. When the non-fixed support (S_1) was moved to the position near the initial crack, the calculated Y_I might be negative because the crack faces experienced a closing rather than an opening mode. Therefore, the negative Y_I and the corresponding Y_{II} and T* should be eliminated. Variations of Y_I, Y_{II} and T* versus S_1/R for different loading conditions and specimen geometries are plotted in Figure 2.

Figure 2 shows that when S_1=S_2, Y_I reaches its maximum while Y_{II} is equal to zero. Y_I decreases while Y_{II} increases with the decrease of S_1 (i.e. S_1 is moved gradually towards the crack plane). When non-fixed bottom support (S_1) is moved to a special position ($S_{1,\text{mode II}}$) near the crack plane, Y_I becomes zero while Y_{II} is non-zero. The larger the crack length ratio is, the closer the special position ($S_{1,\text{ mode II}}$) is to the crack plane. Figure 2(a) also shows that for each value of crack length ratio, there is always a special combination of S_1/R and S_2/R that allow the specimen to be subjected to pure mode II loading, illustrating that the ASCB specimen is capable of covering a full range from pure mode I to pure mode II. Figure 2(c) shows that the normalized T-stress (T*) decreases with the decrease in S_1 and that there exist two positive values. In the light of report by COTTERELL et al [39], both the sign and magnitude of the T-stress exerted a certain degree of influence on the stability of crack propagation. A crack subjected to pure mode I loading propagates steadily along its extension line when the sign of its T-stress is negative, while its propagation may become unstable as the T-stress has a positive value.

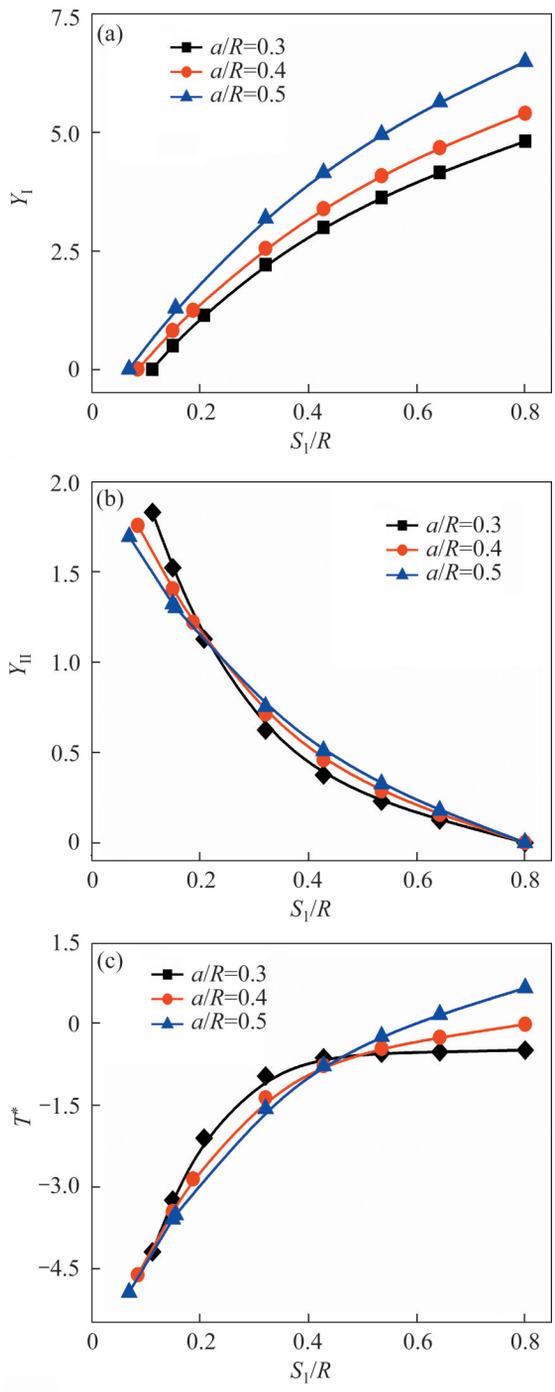

Figure 2 Variations of three crack parameters versus S_1/R for different a/R: (a) Mode I geometry factor; (b) Mode II geometry factor; (c) Normalized T-stress

4 Experimental results

4.1 Mode I/II fracture toughness

Recorded fracture loads and corresponding fracture toughness are listed in Tables 1 − 3. The tested specimens in this work were described by following the sequence "crack length ratio (a/R) - mixity parameter (M^e) -test number". For example, "0.4-0.5" represented a tested sample with a/R=0.4 and M^e=0.5.

Table 1 Fracture loads and corresponding fracture toughness for test samples with a/R=0.3

Specimen	Fracture mode	Fracture load, P_f/kN	K_{IC}/(MPa·m$^{1/2}$)	K_{IIC}/(MPa·m$^{1/2}$)
0.3-0.0-1	Pure mode II	12.32	0	1.84
0.3-0.0-2	Pure mode II	12.59	0	1.91
0.3-0.0-3[a]	Pure mode II	11.77	0	1.79
0.3-0.5-1[a]	Mixed mode	8.64	0.86	0.85
0.3-0.5-2	Mixed mode	9.49	0.95	0.94
0.3-0.5-3	Mixed mode	9.22	0.86	0.86
0.3-0.83-1	Mixed mode	6.70	1.31	0.37
0.3-0.83-2	Mixed mode	6.55	1.28	0.36
0.3-0.83-3	Mixed mode	6.24	1.19	0.33
0.3-0.97-1	Mixed mode	4.75	1.38	0.09
0.3-0.97-2	Mixed mode	4.68	1.39	0.10
0.3-0.97-3	Mixed mode	5.11	1.44	0.10
0.3-1.0-1	Pure mode I	3.99	1.68	0
0.3-1.0-2	Pure mode I	3.58	1.47	0
0.3-1.0-3	Pure mode I	3.91	1.63	0

[a]: an undesired crack occurs in specimen.

Figure 3 shows that when the crack length ratio increases from 0.3 to 0.5, the mean value of the mode I fracture toughness K_{IC} decreases from 1.59 to 1.43 MPa·m$^{1/2}$, and the average value of K_{IIC} decreases from 1.85 to 1.67 MPa·m$^{1/2}$. The values of the mode I/II fracture toughnesses have a slight decrease when the crack length ratio is 0.5. The phenomenon appears to indicate that both K_{IC} and K_{IIC} values obtained from the experiments are dependent on the crack length ratio. As a mechanical parameter of material, however, the fracture toughness should be constant. In this study,

Table 2 Fracture loads and corresponding fracture toughness for test samples with a/R=0.4

Specimen	Fracture mode	Fracture loads, P_f/kN	K_{IC}/(MPa·m$^{1/2}$)	K_{IIC}/(MPa·m$^{1/2}$)
0.4-0.0-1	Pure mode II	10.87	0	1.80
0.4-0.0-2	Pure mode II	10.04	0	1.75
0.4-0.0-3	Pure mode II	9.78	0	1.67
0.4-0.5-1	Mixed mode	10.27	1.23	1.21
0.4-0.5-2	Mixed mode	8.39	1.02	1.00
0.4-0.5-3	Mixed mode	9.57	1.17	1.15
0.4-0.83-1	Mixed mode	5.46	1.37	0.38
0.4-0.83-2	Mixed mode	6.65	1.69	0.47
0.4-0.83-3	Mixed mode	5.31	1.33	0.37
0.4-0.95-1	Mixed mode	3.8	1.51	0.11
0.4-0.95-2	Mixed mode	3.63	1.41	0.10
0.4-0.95-3	Mixed mode	3.47	1.37	0.10
0.4-1.0-1	Pure mode I	2.98	1.55	0
0.4-1.0-2	Pure mode I	2.77	1.46	0
0.4-1.0-3	Pure mode I	2.72	1.44	0

Table 3 Fracture loads and corresponding fracture toughness for test samples with a/R=0.5

Specimen	Fracture mode	Fracture load, P_f/kN	K_{IC}/(MPa·m$^{1/2}$)	K_{IIC}/(MPa·m$^{1/2}$)
0.5-0.0-1	Pure mode II	8.64	0	1.61
0.5-0.0-2	Pure mode II	8.82	0	1.64
0.5-0.0-3	Pure mode II	9.23	0	1.76
0.5-0.5-1	Mixed mode	6.69	0.97	0.97
0.5-0.5-2	Mixed mode	6.77	0.95	0.96
0.5-0.5-3	Mixed mode	7.16	1.04	1.05
0.5-0.85-1	Mixed mode	3.50	1.22	0.29
0.5-0.85-2	Mixed mode	3.96	1.41	0.33
0.5-0.85-3	Mixed mode	3.39	1.21	0.28
0.5-0.96-1	Mixed mode	2.64	1.46	0.09
0.5-0.96-2	Mixed mode	2.51	1.38	0.09
0.5-0.96-3	Mixed mode	2.83	1.54	0.1
0.5-1.0-1	Pure mode I	2.13	1.47	0
0.5-1.0-2	Pure mode I	2.04	1.49	0
0.5-1.0-3	Pure mode I	1.88	1.34	0

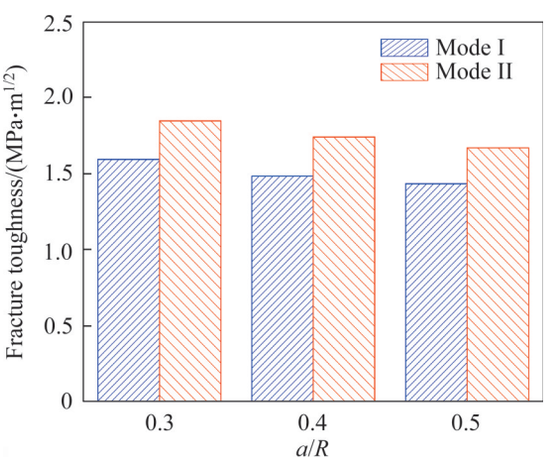

Figure 3 Effect of crack length ratio on fracture toughness

both the mode-I and mode-II fracture toughnesses decrease by 10%. The changes in the mode I fracture resistance shown in Figure 3 are similar to the findings from the previous studies [40−43]. The reason for the deviation may be due to the influence of fracture process zone [44]. As we known, the typical calculation of fracture toughness is based on the linear elastic fracture mechanics; however, rock is a heterogeneous material and often performs non-linear characteristics. For the specimen with large notch length, it has a short ligament length, and the fracture process zone will have a great influence on the fracture properties of rock.

4.2 Mixed fracture criteria

Several mixed mode fracture criteria have been proposed to investigate the onset of fracture and direction of crack propagation in rock materials

subjected to a mixed mode loading. The maximum energy release rate (G_{max}) criterion [45 – 47], the minimum strain energy density (S_{min}) criterion [48] and the maximum tangential stress (MTS) criterion [49] are the most commonly used mixed mode fracture criteria. All of them utilize the stress field existing just before the onset of crack propagation [50]. Defining r and θ as shown in Figure 4, the stress field near crack tip for a homogeneous and isotropic linear elastic material in polar co-ordinates is defined as [51]:

$$\begin{cases}\sigma_{rr}=\dfrac{1}{\sqrt{2\pi r}}\cos\left(\dfrac{\theta}{2}\right)\left[K_{\mathrm{I}}\left(1+\sin^2\left(\dfrac{\theta}{2}\right)\right)+\right.\\ \left.\dfrac{3}{2}K_{\mathrm{II}}\left(\sin\theta-2\tan\left(\dfrac{\theta}{2}\right)\right)\right]+T\cos^2\theta+O\left(\sqrt{r}\right)\\ \sigma_{\theta\theta}=\dfrac{1}{\sqrt{2\pi r}}\cos\left(\dfrac{\theta}{2}\right)\left(K_{\mathrm{I}}\cos^2\left(\dfrac{\theta}{2}\right)-\dfrac{3}{2}K_{\mathrm{II}}\sin\theta\right)+\\ T\sin^2\theta+O\left(\sqrt{r}\right)\\ \tau_{r\theta}=\dfrac{1}{\sqrt{2\pi r}}\cos\left(\dfrac{\theta}{2}\right)\left[K_{\mathrm{I}}\sin\theta+K_{\mathrm{II}}(3\cos\theta-1)\right]-\\ T\sin\theta\cos\theta+O\left(\sqrt{r}\right)\end{cases} \tag{2}$$

where K_{I}, K_{II} and T denote the SIFs of modes I and II and T-stress, respectively; O is the usual Landau symbol.

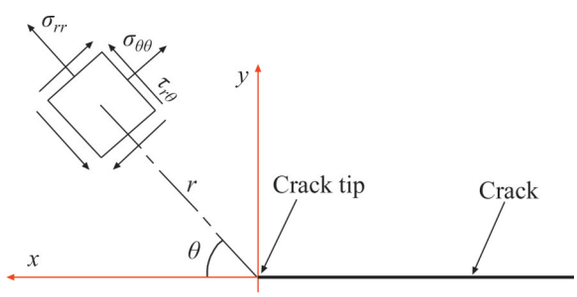

Figure 4 Stress field in polar co-ordinate system

The MTS criterion is the simplest and thus is used more frequently by researchers. It states that crack propagation initiates radially from the crack tip in a plane perpendicular to the direction of the maximum tangential tensile stress and that a new crack occurs when the maximum tangential stress reaches a critical value. In terms of the MTS criterion, the crack initiation angle and onset of fracture can be given respectively by:

$$\cos\left(\frac{\theta_o}{2}\right)\left[K_{\mathrm{I}}\sin\theta_o+K_{\mathrm{II}}\left(3\cos\theta_o-1\right)\right]=0 \tag{3}$$

and

$$\cos\left(\frac{\theta_o}{2}\right)\left(\frac{K_{\mathrm{I}}}{K_{\mathrm{IC}}}\cos^2\left(\frac{\theta_o}{2}\right)-3\frac{K_{\mathrm{II}}}{K_{\mathrm{IC}}}\sin\theta_o\right)=1 \tag{4}$$

where θ_O is defined as the crack initiation angle. For a pure mode II crack problem, K_{I}=0, θ_{II}=70.5° and $K_{\mathrm{IIC}}/K_{\mathrm{IC}}$=0.87.

However, some researchers [27, 52, 53] found that the crack initiation angle and onset of fracture predicted with the conventional MTS criterion were not in good agreement with their experimental observations. In this situation, SMITH et al [54] first introduced the generalized MTS (GMTS) criterion (also known as the modified MTS criterion) which takes into account the effects of T-stress on the original basis. In terms of the GMTS criterion, the direction of fracture initiation (θ_O) can be determined from [54]:

$$K_{\mathrm{I}}\sin\theta_o+K_{\mathrm{II}}\left(3\cos\theta_o-1\right)-\frac{16T}{3}\sqrt{2\pi r_{\mathrm{c}}}\cos\theta_o\sin\left(\frac{\theta_o}{2}\right)=0 \tag{5}$$

where r_{c} is defined as the radius of the fracture process zone which is considered to be a material constant. Substituting Eq. (1) into Eq. (5) yields:

$$Y_{\mathrm{I}}\sin\theta_o+Y_{\mathrm{II}}\left(3\cos\theta_o-1\right)-\frac{16T^*}{3}\sqrt{\frac{2r_{\mathrm{c}}}{a}}\cos\theta_o\sin\left(\frac{\theta_o}{2}\right)=0 \tag{6}$$

The results of the mixed mode fracture toughness are commonly shown in the normalized form of $K_{\mathrm{II}}/K_{\mathrm{IC}}$ and $K_{\mathrm{I}}/K_{\mathrm{IC}}$ [54]. According to the GMTS criterion and AYATOLLAHI et al's study [27], the ratios $K_{\mathrm{I}}/K_{\mathrm{IC}}$ and $K_{\mathrm{II}}/K_{\mathrm{IC}}$ for the ASCB specimen subjected to mixed mode loading can be written in terms of Y_{II}, Y_{II} and T* as:

$$\frac{K_{\mathrm{I}}}{K_{\mathrm{IC}}}=\left[\cos\left(\frac{\theta_o}{2}\right)\left(\cos^2\left(\frac{\theta_o}{2}\right)-\frac{3}{2}\frac{Y_{\mathrm{II}}}{Y_{\mathrm{I}}}\sin\theta_o\right)+\sqrt{\frac{2r_{\mathrm{c}}}{a}}\frac{T^*}{Y_{\mathrm{I}}}\sin^2\theta_o\right]^{-1} \tag{7}$$

and

$$\frac{K_{II}}{K_{IC}}=\left[\cos\left(\frac{\theta_o}{2}\right)\left(\frac{Y_I}{Y_{II}}\cos^2\left(\frac{\theta_o}{2}\right)-\frac{3}{2}\sin\theta_o\right)+\sqrt{\frac{2r_c}{a}}\frac{T^*}{Y_{II}}\sin^2\theta_o\right]^{-1} \quad (8)$$

The K_I/K_{IC} and K_{II}/K_{IC} ratios are determined by substituting the crack initiation angle (θ_o) obtained and the values of Y_{II}, Y_{II} and T* into Eqs. (7) and (8). It is found from Eqs. (5)−(8) that the selection of an appropriate value of r_c plays a crucial role in the use of GMTS criterion.

In this study, the dimension of r_c for rock materials is determined in terms of SCHMIDT's suggestion [55] by the following formula:

$$r_c=\frac{1}{2\pi}\left(\frac{K_{IC}}{\sigma_t}\right)^2 \quad (9)$$

where r_c is then calculated as 2.6 mm by substituting the mode I fracture toughness of 1.50 MPa·m$^{1/2}$ and the tensile strength of 11.73 MPa into Eq. (9). It is noted that the value of K_{IC} is calculated by averaging all the results obtained from different crack length ratios for the specimens tested.

4.3 Mixed mode fracture toughness

There is a preference for researchers [41, 56] in the field of rock mechanics to present the results of the mixed-mode fracture toughnesses in the normalized forms of K_I/K_{IC} and K_{II}/K_{IC}. The mode I fracture toughness K_{IC} is calculated to be about 1.50 MPa·m$^{1/2}$ by averaging all the results obtained from the pure mode I tests. The comparison shown in Figure 5 illustrates the S_{min} criterion is closer to the experimental data, but still fails to provide an adequate fit. As mentioned earlier, both the G_{max} and MTS criteria are independent of material properties, while the S_{min} criterion is the only one that is dependent on the material properties such as Poisson ratio. The criterion dependent on material properties seems to provide more reasonably predicted results, in comparison with those independent of material properties. If so, it is necessary to present the predicted results of the GMTS criterion because the criterion is also influenced by variations in material properties represented by the tensile strength and mode I fracture toughness.

It can be seen from Figure 6 that experimental

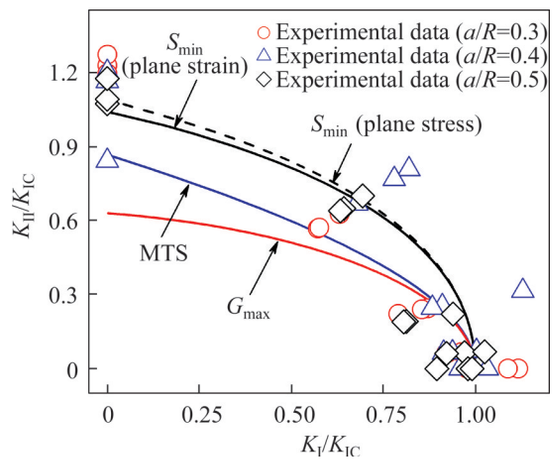

Figure 5 Comparison of experimental data with three classical fracture criteria of S_{min}, G_{max} and MTS

data are not completely consistent with the GMTS criterion curves, although the criterion takes into account the effect of the non-singular stress term (i.e. T-stress) in addition to the singular stress terms. Note that in terms of the GMTS criterion, the changes in the crack length ratio have a negligible effect on its curve shape, and the curves shown in Figure 6 only consider the effect of the crack length ratio of 0.3.

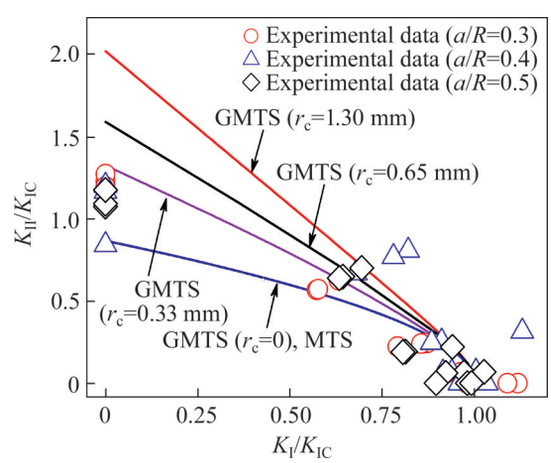

Figure 6 Comparison of experimental data with GMTS criterion

The fracture toughness ratio (K_{IIC}/K_{IC}) is an excellent indicator of the availability of mixed-mode fracture criterion [29, 56]. AYATOLLAHI et al [56] even suggested that the extra efforts and expenses in performing pure mode II fracture tests can be omitted, as long as the fracture toughness (K_{IC}) and an appropriate mixed mode criterion for predicting the fracture toughness ratio (K_{IIC}/K_{IC}) are

provided. The fracture toughnesses K_{IC} and K_{IIC} for the tested samples are measured to be 1.50 and 1.75 MPa·m$^{1/2}$, respectively, by averaging the results obtained from the pure mode I and II tests. The fracture toughness ratio K_{IIC}/K_{IC} is then determined to be 1.17.

Table 4 summarizes some of the K_{IIC}/K_{IC} ratios predicted by various criteria and experimental results. Clearly, there is a wide range of K_{IIC}/K_{IC} ratio predicted by different criteria. It seems that the fracture toughness ratio predicted by the S_{min} criterion under plane stress conditions is closer to the experimental results, compared with other mixed-mode criteria. LIM et al [29] summed up some K_{IIC}/K_{IC} ratios of rock materials and showed that they varied between 0.32 and 3.59. Moreover, AYATOLLAHI et al [56] made a review of fracture toughness ratios of various rock materials and then found that they ranged from 1.13 to 2.19. Also, they developed a new and more accurate approach based on the MTS criterion to estimate the K_{IIC}/K_{IC} ratio of brittle materials. In view of the fact that the Poisson ratio for most rocks lies between 0.2 and 0.4, the K_{IIC}/K_{IC} ratio predicted by the S_{min} criterion is in the range of 0.76 – 1.02. These different ranges suggest that the universal applicability of the S_{min} criterion dependent on the material Poisson ratio should be discussed further.

Table 4 Fracture toughness ratios predicted by varying mixed mode fracture criteria and experimental result

Fracture criterion	K_{IIC}/K_{IC}	Source
G_{max}	0.87	PALANISWAMY et al [45]
	0.63	HUSSAIN et al [46]
	0.75	UEDA [47]
MTS	0.87	ERDOGAN et al [49]
GMTS (r_c=2.60 mm)	2.39	SMITH et al [54]
GMTS (r_c=1.30 mm)	2.02	
GMTS (r_c=0.65 mm)	1.59	
GMTS (r_c=0.33 mm)	1.32	
S_{min} (Plane stress, v=0.23)	1.04	SIH [48]
S_{min} (Plane strain, v=0.23)	0.99	SIH [48]
Experimental result	1.17	This work

4.4 Crack initiation angle

Sufficient knowledge of the crack initiation angle is indispensable for the study of path of crack growth and is as important as that of the onset of fracture [50]. The crack initiation angle involving mixed-mode fracture of brittle materials has been widely investigated by researchers, and several criteria based on stress, strain and energy have been proposed [50, 53, 57].

The x axis in Figure 8 is represented by the mixity parameter M^e [53, 54] as:

$$M^e = \frac{2}{\pi}\tan^{-1}\left(\frac{K_I}{K_{II}}\right) \tag{10}$$

where M^e varies from zero (for pure mode II) to 1 (for pure mode I) [54]. The crack initiation angle is measured clockwise from the center line of the specimen, as shown in Figure 7. An observation on the final fracture paths of some samples shows that the crack front tends to do not propagate equally throughout the thickness of the specimen, probably due to non-uniform distribution of forces or heterogeneities within the specimen. Therefore, the crack initiation angle presented in Figure 8 is an average fracture angle of both sides of the fractured specimen.

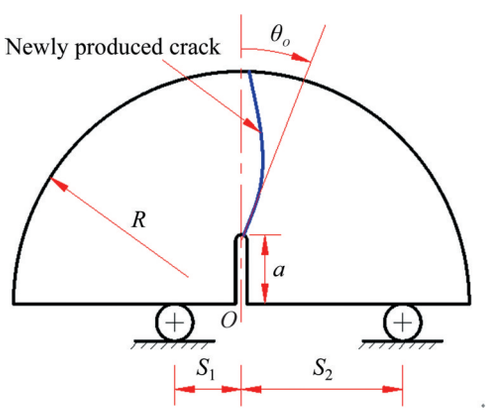

Figure 7 Measurement method for crack initiation angle

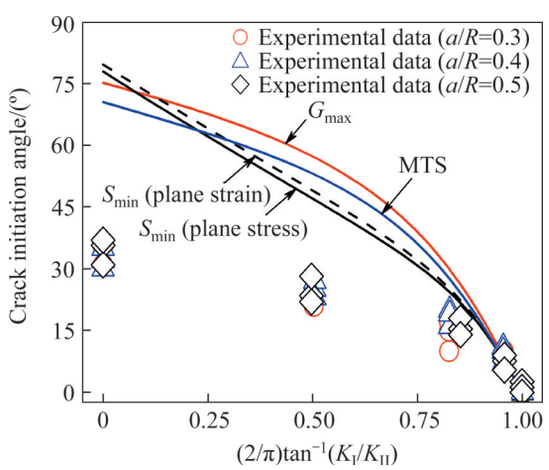

Figure 8 Comparison of three classical criteria curves and experimentally determined crack initiation angles

Figure 8 shows that theoretical predictions are not consistent with the experimental data completely. It seems that the existing mixed mode fracture criterion which only employs singular stress terms and ignores the influence of the *T*-stress fails to provide a reasonable prediction for the experimentally determined crack initiation angle, while the GMTS criterion improves the accuracy of stress calculations ahead of a crack tip by considering the effect of *T*-stress on the original basis. Therefore, an examination of the effect of *T*-stress on fracture angle is necessary.

It is found from Figure 9 that there is a good agreement between the GMTS criterion with r_c=2.6 mm and experimental data, illustrating that the criterion provides a more reasonable prediction for the crack initiation angle compared with those conventional criteria. Also, it can be seen from the curves for the GMTS criterion with r_c=2.6 mm that the crack length ratio (a/R) has a negligible effect on the GMTS curves, but the value of r_c has a significant influence. Accordingly, we only use the crack length ratio of 0.3 to calculate other GMTS curves by solving Eq. (6). The lower the value of r_c is, the closer the GMTS curves are to the MTS curve, and when r_c=0, both curves are identical.

4.5 Crack propagation path

Figure 10 illustrates the fractured ASCB specimens under varying combinations of modes I and II. Note that only a single crack occurs in a tested specimen, as shown in Figure 10. Unlike in a rock plate containing an inclined flaw under compression [58, 59], there is no quasi coplanar or oblique secondary crack within the fractured ASCB specimen. It is suggested that the use of the ASCB specimen for determining mode I or mixed-mode fracture toughness may have more advantages in terms of stability and reliability compared with the cracked chevron-notched Brazilian disc or cracked straight through Brazilian disc specimen, in both of which two cracks nucleate around the tips of a pre-existing flaw.

In this study, the fracture propagation process of the sample was investigated using digital image correlation and high-speed camera techniques. Owing to the interframe time of the high-speed camera set to 20 μs, the loading time of the testing lasts 150−200 s. The camera has no enough memory to record the total testing process. Therefore, only the initiation and propagation of the crack in front of the notch tip and the macro-failure of the sample were recorded. Figure 11 shows the pure mode I, mixed mode and pure mode II crack growth trajectories of ASCB specimens. It is noted that the value around the red arrow is the time increment between two close subplots. The sizes of zone-of-interest (white dotted line in Figure 11) of 14.5 cm× 14.5 cm were selected for correlation calculation. It is found that every newly produced crack initiates at the flaw tip. As shown in Figure 11(a), it is found that when the ASCB specimen is subjected to pure mode I loading, a crack emanates from the tip of the flaw and propagates exactly straight along the extended line of the flaw till the specimen fails completely. As mentioned earlier, mode II is becoming a dominant effect when the non-fixed support (S_1) is gradually moved towards the crack.

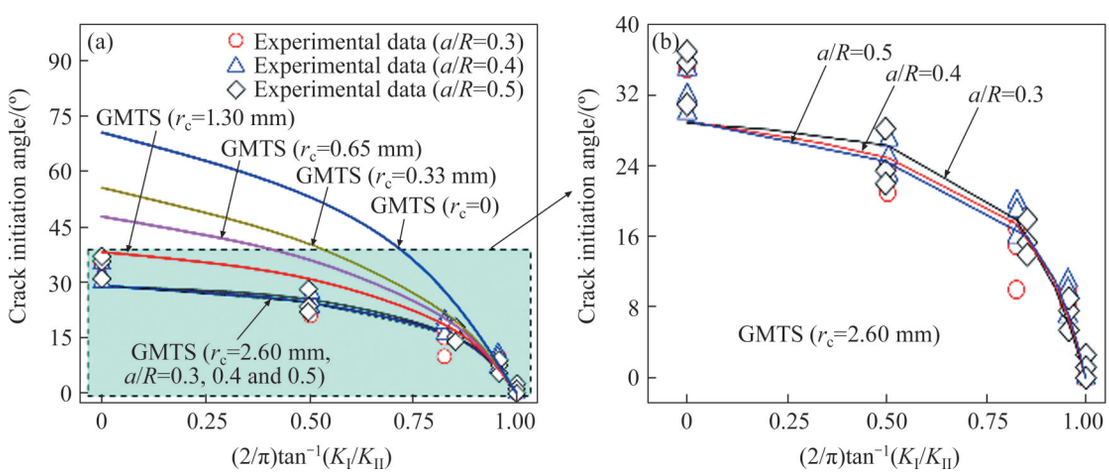

Figure 9 Comparison of experimentally determined crack initiation angles (a) with different values of r_c and curves of GMTS criterion (b)

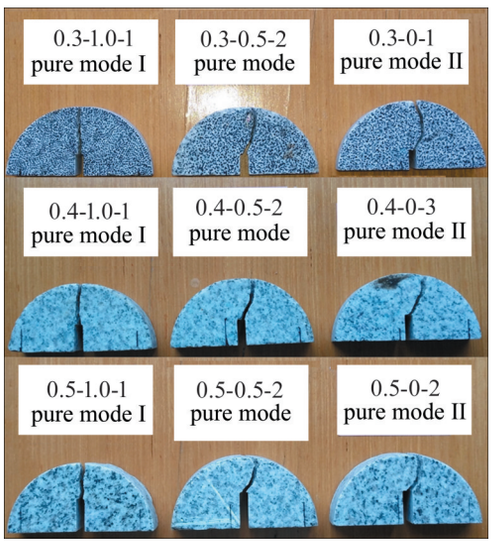

Figure 10 Fractured ASCB specimens

In this circumstance, a crack initiates at an angle to the original flaw line around the tip of a flaw, then propagates along a curvilinear path, and finally grows to the position near the loading point on the specimen, as shown in Figures 11(b) and (c). Moreover, it is found that the fracture process zone develops ahead of the crack tip, and then propagates toward the loading end with the increase of applied load.

The above observations illustrate that there is an advantage of the use of the ASCB specimen for fracture toughness determination of rock materials over the SCB specimen application. A review of previous studies revealed that the crack in the SCB specimen tended to emanate from the tip of pre-existing flaw when its inclination angle was low, while the fracture initiation point might occur behind the flaw tip with the increasing flaw inclination angle. For example, there were several undesired fracture initiation points in works by LIM et al [29] on a water-saturated synthetic mudstone, when the flaw inclination angles in the SCB specimen were greater than 50° . The abnormal fracture point exerted more or less influence upon the stability and dependability of the SCB specimen used to determine the fracture resistance of rock materials, although they argued that it would not affect significantly the final results.

5 Improvement for ASCB test

A review of the literature related to the before specimens indicates that simple geometry and loading configuration, easily extracting from rock cores and low cost are the main reasons for their

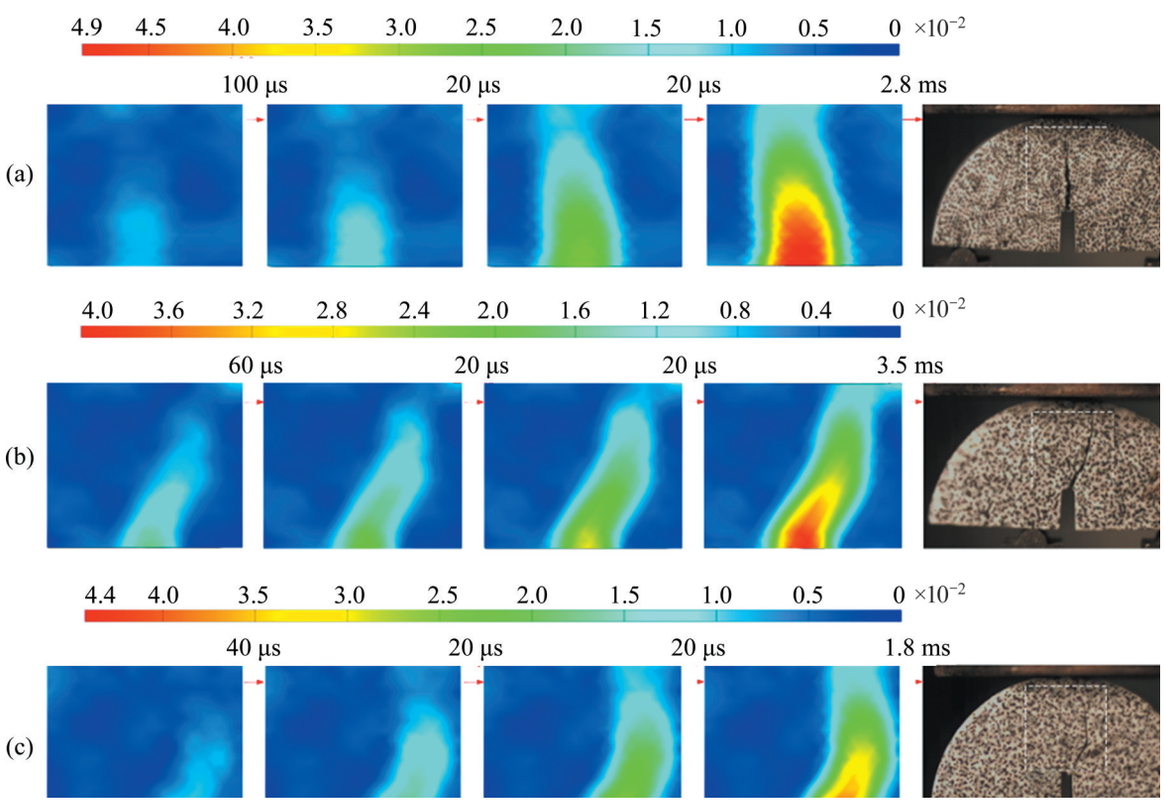

Figure 11 Pure mode I (a), mixed mode (b) and pure mode II (c) fracture processes of specimens with a/R=0.3

extensive application. However, note that there are some limitations in the process of their implementations that even prevent them to cover full range of mixed mode loading from pure mode I to pure mode II [30]. For example, for the conventional SCB specimen with low crack length ratio, its pure mode-II loading condition may be obtained at a large flaw inclination angle. However, the unwanted fracture may occur during the machining process of the initial flaw with an inclination angle greater than 50° [29]. For the specimen with a larger crack length ratio, pure mode II loading condition can be met at a low flaw inclination angle. In this case, two potential problems arise that the ligament length of the specimen may be less than the size of fracture process zone and the undesired fracture initiation point away from the crack tip may occur during testing. To eliminate the above shortcomings, AYATOLLAHI et al [30] proposed the improved SCB specimen, namely the ASCB specimen, to investigate the cracking behavior in brittle materials.

The ASCB specimen has already been used successfully to investigate the cracking behavior in poly methyl methacrylate (PMMA) [30]. The aim of the present study is to extend the use of the ASCB specimen for fracture resistance determination of rock materials. A series of fracture tests were performed by using the ASCB specimens manufactured from Granite. The specimen has attracted wide attention due to its outstanding advantages which had been summarized by AYATOLLAHI et al [30]. However, certain shortcomings of the ASCB specimen should be paid attention to in practical application.

Mode mixities in the ASCB specimen are too sensitive to the non-fixed support ratio (S_1/R), particularly under mode II dominant loading conditions. This potential problem cannot be found from Figures 2(a) and (b). Figure 12 shows variations of the mixity parameter M^e versus the bottom support ratio (S_1/R). It can be found that the slopes of M^e curve decrease with the increase in S_1/R. More specifically, when the S_1/R range is between 0.23 and 0.07 (pure mode II), M^e approximately accounts for 60% of the total value, whereas the rest of M^e is influenced by the value of S_1/R ranging from 0.23 to 0.8 (pure mode I). This means a slight misalignment of the non-fixed bottom support (S_1/R) may induce a component of mode I loading to occur and pure mode II loading cannot be achieved. Nevertheless, the control over the non-fixed bottom support for the ASCB specimen is easier than producing an initial flaw with a large inclination angle in the SCB specimen.

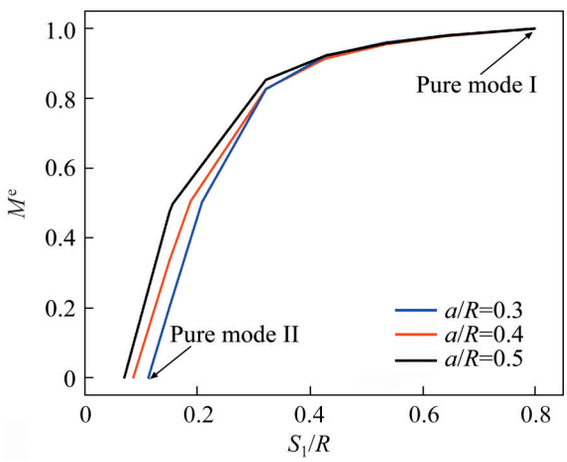

Figure 12 Variations of M^e with S_1/R

There is still undesired fracture during testing. Figure 13 shows two fractured samples with undesired cracks. The crack initiation point in the ASCB specimen should be located close to the tip of pre-existing flaw, where the maximum tensile stress is attained. However, when performing fracture tests on the specimens with a/R=0.3 under mode II dominant loading conditions, we observed some newly produced cracks initiated from the vicinity of the contact point between the non-fixed bottom support (S_1/R) and the specimen. However, for the specimens with a/R=0.4 and 0.5, normal crack initiation points occurred during testing. This comparison illustrates that the stress concentration near the contact point is responsible for the undesired fracture. Note that crack initiation point

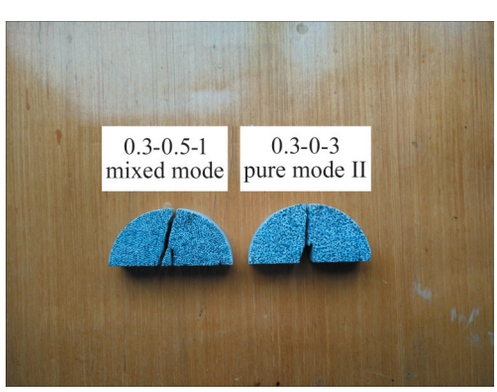

Figure 13 Undesired fractured specimens

only occurred in one of the three specimens with S_1/R=0.3 − 0.0 (pure mode II), and the other two fractured normally. The situation for specimens with S_1/R=0.3 − 0.5 was the same as for specimens with S_1/R=0.3 − 0.0. The reason for this difference might be that heterogeneities and natural fractures within the specimen were involved in the determination of the fracture resistance. Clearly, it is a better choice to use the ASCB specimen with a higher crack length ratio to perform fracture tests on rock materials. In this case, a problem arises that whether the ligament length of the specimen is less than the size of r_c. Therefore, more research is needed to find a balance point between the two, but this is outside the scope of this article.

6 Conclusions

In this paper, we extend the use of the ASCB specimen, to investigate the cracking behavior within rock materials, in the hope of obtaining a deeper understanding of its application. This study conducts the detailed analysis to the onset of fracture, crack initiation angle and crack propagating trajectory, combined with several mixed-mode fracture criteria. However, it should be noted that there are still some limitations in our work: only one type of rock material, granite, is chosen to perform fracture tests; there is a superfluity of fracture tests in this work under mode I dominant loading conditions (i.e. M^e>0.5), but a few under mode II dominant loading conditions (i.e. M^e<0.5); the reason for undesired fractures during testing is analyzed briefly. Further researches will remove the limitations above, and the following conclusions are obtained.

1) Both the mode-I and mode-II fracture toughnesses have a slight decrease with the increase of the crack length ratio. The mean fracture toughnesses K_{IC} and K_{IIC} for the tested granite samples are 1.50 and 1.75 MP·am$^{1/2}$, respectively. The fracture toughness ratio K_{IIC}/K_{IC} is 1.17.

2) A comparison between the experimental results and curves for the mixed mode fracture criteria shows that among the four criteria, the minimum strain energy density (S_{min}) criterion is the closest to the experimental results. However, the generalized maximum tangential stress (GMTS) criterion with the fracture process zone length of 2.6 mm agrees well with the crack initiation angles.

3) When the specimen with a low crack length ratio is applied to preform fracture test, the crack initiation point may occur close to the contact point between specimen and the non-fixed bottom support (S_1/R). Because of local stress concentration, the specimen with a higher crack length ratio fractures as expected. Therefore, the use of the ASCB specimen with a higher crack length ratio for fracture resistance determination of rock materials is a better choice.

Contributors

WU Qiu-hong provided the concept and edited the draft of manuscript. XIE You-sheng conducted the literature review and wrote the first draft of the manuscript. LIU Jie and WENG Lei analyzed the measured data. ZHAO Yan-lin and LI Xue-feng edited the draft of manuscript. XIE Cheng-long conducted numerical simulations. All authors replied to reviewers' comments and revised the final version.

Conflict of interest

WU Qiu-hong, XIE Cheng-long, XIE You-sheng, ZHAO Yan-lin, LI Xue-feng, LIU Jie and WENG Lei declare that they have no conflict of interest.

References

[1] WU Qiu-hong, WENG Lei, ZHAO Yan-lin, et al. Influence of infilling stiffness on mechanical and fracturing responses of hollow cylindrical sandstone under uniaxial compression tests [J]. Journal of Central South University, 2021, 28(8): 2485−2498. DOI: 10.1007/s11771-021-4781-z.

[2] JIA P, YANG T H, YU Q L. Mechanism of parallel fractures around deep underground excavations [J]. Theoretical and Applied Fracture Mechanics, 2012, 61: 57−65. DOI: 10.1016/j.tafmec.2012.08.007.

[3] BIDGOLI M N, ZHAO Zhi-hong, JING Lan-ru. Numerical evaluation of strength and deformability of fractured rocks [J]. Journal of Rock Mechanics and Geotechnical Engineering, 2013, 5(6): 419 − 430. DOI: 10.1016/j. jrmge. 2013.09.002.

[4] PAKDAMAN A M, MOOSAVI M, MOHAMMADI S. Experimental and numerical investigation into the methods of determination of mode I static fracture toughness of rocks [J]. Theoretical and Applied Fracture Mechanics, 2019, 100: 154−170. DOI: 10.1016/j.tafmec.2019.01.001.

[5] OUCHTERLONY F. Suggested methods for determining the fracture toughness of rock [J]. International Journal of Rock

Mechanics and Mining Sciences & Geomechanics Abstracts, 1988, 25(2): 71−96. DOI: 10.1016/0148-9062(88)91871-2.

[6] BUSH A J. Experimentally determined stress-intensity factors for single-edge-crack round bars loaded in bending [J]. Experimental Mechanics, 1976, 16(7): 249 − 257. DOI: 10.1007/BF02321148.

[7] CHONG K P, KURUPPU M D. New specimens for mixed mode fracture investigations of geomaterials [J]. Engineering Fracture Mechanics, 1988, 30(5): 701 − 712. DOI: 10.1016/0013-7944(88)90160-9.

[8] KURUPPU M D, OBARA Y, AYATOLLAHI M R, et al. ISRM-suggested method for determining the mode I static fracture toughness using semi-circular bend specimen [J]. Rock Mechanics and Rock Engineering, 2014, 47(1): 267 − 274. DOI: 10.1007/s00603-013-0422-7.

[9] KURUPPU M. Fracture toughness measurement using chevron notched semi-circular bend specimen [J]. International Journal of Fracture, 1997, 86(4): L33−L38.

[10] AWAJI H, SATO S. Combined mode fracture toughness measurement by the disk test [J]. Journal of Engineering Materials and Technology, 1978, 100(2): 175 − 182. DOI: 10.1115/1.3443468.

[11] WANG Qi-zhi, XING Lei. Determination of fracture toughness KIC by using the flattened Brazilian disk specimen for rocks [J]. Engineering Fracture Mechanics, 1999, 64(2): 193 − 201. DOI: 10.1016/S0013-7944(99)00065-X.

[12] PEI Peng-da, DAI Feng, LIU Yi, et al. Dynamic tensile behavior of rocks under static pre-tension using the flattened Brazilian disc method [J]. International Journal of Rock Mechanics and Mining Sciences, 2020, 126: 104208. DOI: 10.1016/j.ijrmms.2019.104208.

[13] FOWELL R J. Suggested method for determining mode I fracture toughness using cracked chevron notched Brazilian disc (CCNBD) specimens [J]. International Journal of Rock Mechanics and Mining Sciences & Geomechanics Abstracts, 1995, 32(1): 57−64. DOI: 10.1016/0148-9062(94)00015-U.

[14] YANG S, TANG Tian-xi, ZOLLINGER D G, et al. Splitting tension tests to determine concrete fracture parameters by peak-load method [J]. Advanced Cement Based Materials, 1997, 5(1): 18−28. DOI: 10.1016/S1065-7355(97)90011-0.

[15] ALIHA M R M, BAHMANI A. Rock fracture toughness study under mixed mode I/III loading [J]. Rock Mechanics and Rock Engineering, 2017, 50(7): 1739 − 1751. DOI: 10.1007/s00603-017-1201-7.

[16] ALIHA M R M, SARBIJAN M J, BAHMANI A. Fracture toughness determination of modified HMA mixtures with two novel disc shape configurations [J]. Construction and Building Materials, 2017, 155: 789 − 799. DOI: 10.1016/j.conbuildmat.2017.08.093.

[17] BAHMANI A, FARAHMAND F, JANBAZ M R, et al. On the comparison of two mixed-mode I + III fracture test specimens [J]. Engineering Fracture Mechanics, 2021, 241: 107434. DOI: 10.1016/j.engfracmech.2020.107434.

[18] TANG Tian-xi, BAŽANT Z P, YANG S, et al. Variable-Notch one-size test method for fracture energy and process zone length [J]. Engineering Fracture Mechanics, 1996, 55(3): 383−404. DOI: 10.1016/0013-7944(96)00030-6.

[19] WENG Lei, WU Qiu-hong, ZHAO Yan-lin, et al. Dynamic response and failure of rock in initial gradient stress field under stress wave loading [J]. Journal of Central South University, 2020, 27(3): 963 − 972. DOI: https://doi.org/10.1007/s11771-020-4344-8.

[20] WU Qiu-hong, CHEN Lu, SHEN Bao-tang, et al. Experimental investigation on rockbolt performance under the tension load [J]. Rock Mechanics and Rock Engineering, 2019, 52(11): 4605 − 4618. DOI: 10.1007/s00603-019-01845-1.

[21] WU Qiu-hong, WENG Lei, ZHAO Yan-lin, et al. On the tensile mechanical characteristics of fine-grained granite after heating/cooling treatments with different cooling rates [J]. Engineering Geology, 2019, 253: 94−110. DOI: 10.1016/j.enggeo.2019.03.014.

[22] AMERI M, MANSOURIAN A, PIRMOHAMMAD S, et al. Mixed mode fracture resistance of asphalt concrete mixtures [J]. Engineering Fracture Mechanics, 2012, 93: 153 − 167. DOI: 10.1016/j.engfracmech.2012.06.015.

[23] FATTAHI AMIRDEHI H R, ALIHA M R M, MONIRI A, et al. Using the generalized maximum tangential stress criterion to predict mode II fracture of hot mix asphalt in terms of mode I results—A statistical analysis [J]. Construction and Building Materials, 2019, 213: 483 − 491. DOI: 10.1016/j.conbuildmat.2019.04.067.

[24] ALIHA M R M, HOSSEINPOUR G R, AYATOLLAHI M R. Application of cracked triangular specimen subjected to three-point bending for investigating fracture behavior of rock materials [J]. Rock Mechanics and Rock Engineering, 2013, 46(5): 1023−1034. DOI: 10.1007/s00603-012-0325-z.

[25] TUTLUOGLU L, KELES C. Mode I fracture toughness determination with straight notched disk bending method [J]. International Journal of Rock Mechanics and Mining Sciences, 2011, 48(8): 1248 − 1261. DOI: 10.1016/j.ijrmms.2011.09.019.

[26] LIM I L, JOHNSTON I W, CHOI S K. Stress intensity factors for semi-circular specimens under three-point bending [J]. Engineering Fracture Mechanics, 1993, 44(3): 363−382. DOI: 10.1016/0013-7944(93)90030-V.

[27] AYATOLLAHI M R, ALIHA M R M, HASSANI M M. Mixed mode brittle fracture in PMMA—An experimental study using SCB specimens [J]. Materials Science and Engineering A, 2006, 417(1, 2): 348 − 356. DOI: 10.1016/j.msea.2005.11.002.

[28] AYATOLLAHI M R, ALIHA M R M. Wide range data for crack tip parameters in two disc-type specimens under mixed mode loading [J]. Computational Materials Science, 2007, 38(4): 660−670. DOI: 10.1016/j.commatsci.2006.04.008.

[29] LIM I L, JOHNSTON I W, CHOI S K, et al. Fracture testing of a soft rock with semi-circular specimens under three-point bending. Part 1—mode I [J]. International Journal of Rock Mechanics and Mining Sciences & Geomechanics Abstracts, 1994, 31(3): 185−197. DOI: 10.1016/0148-9062(94)90463-4.

[30] AYATOLLAHI M R, ALIHA M R M, SAGHAFI H. An improved semi-circular bend specimen for investigating mixed mode brittle fracture [J]. Engineering Fracture Mechanics, 2011, 78(1): 110 − 123. DOI: 10.1016/j.engfracmech.2010.10.001.

[31] MARSAVINA L, CONSTANTINESCU D M, LINUL E, et al. Refinements on fracture toughness of PUR foams [J].

Engineering Fracture Mechanics, 2014, 129: 54 – 66. DOI: 10.1016/j.engfracmech.2013.12.006.

[32] ALIHA M R M, BEHBAHANI H, FAZAELI H, et al. Study of characteristic specification on mixed mode fracture toughness of asphalt mixtures [J]. Construction and Building Materials, 2014, 54: 623 – 635. DOI: 10.1016/j. conbuildmat. 2013.12.097.

[33] ALIHA M R M, RAZMI A, MANSOURIAN A. The influence of natural and synthetic fibers on low temperature mixed mode I + II fracture behavior of warm mix asphalt (WMA) materials [J]. Engineering Fracture Mechanics, 2017, 182: 322 – 336. DOI: 10.1016/j. engfracmech. 2017. 06.003.

[34] ALIHA M R M. On predicting mode II fracture toughness (K_{IIC}) of hot mix asphalt mixtures using the strain energy density criterion [J]. Theoretical and Applied Fracture Mechanics, 2019, 99: 36 – 43. DOI: 10.1016/j. tafmec. 2018. 11.001.

[35] FAKHRI M, AMOOSOLTANI E, ALIHA M R M. Crack behavior analysis of roller compacted concrete mixtures containing reclaimed asphalt pavement and crumb rubber [J]. Engineering Fracture Mechanics, 2017, 180: 43 – 59. DOI: 10.1016/j.engfracmech.2017.05.011.

[36] RAZAVI S M J, ALIHA M R M, BERTO F. Application of an average strain energy density criterion to obtain the mixed mode fracture load of granite rock tested with the cracked asymmetric four-point bend specimens [J]. Theoretical and Applied Fracture Mechanics, 2018, 97: 419 – 425. DOI: 10. 1016/j.tafmec.2017.07.004.

[37] WANG Yu-suo, HU Xiao-zhi. Determination of tensile strength and fracture toughness of granite using notched three-point-bend samples [J]. Rock Mechanics and Rock Engineering, 2017, 50(1): 17−28. DOI: 10.1007/s00603-016-1098-6.

[38] WENG Lei, LI Xi-bing, TAHERI A, et al. Fracture evolution around a cavity in brittle rock under uniaxial compression and coupled static – dynamic loads [J]. Rock Mechanics and Rock Engineering, 2018, 51(2): 531 – 545. DOI: 10.1007/s00603-017-1343-7.

[39] COTTERELL B, RICE J R. Slightly curved or kinked cracks [J]. International Journal of Fracture, 1980, 16(2): 155 – 169. DOI: 10.1007/BF00012619.

[40] KHAN K, AL-SHAYEA N A. Effect of specimen geometry and testing method on mixed mode I−II fracture toughness of a limestone rock from Saudi Arabia [J]. Rock Mechanics and Rock Engineering, 2000, 33(3): 179 – 206. DOI: 10.1007/s006030070006.

[41] CHANG S H, LEE C I, JEON S. Measurement of rock fracture toughness under modes I and II and mixed-mode conditions by using disc-type specimens [J]. Engineering Geology, 2002, 66(1, 2): 79 – 97. DOI: 10.1016/S0013-7952(02)00033-9.

[42] WANG Jun-jie, HUANG Shi-yuan, GUO Wan-li, et al. Experimental study on fracture toughness of a compacted clay using semi-circular bend specimen [J]. Engineering Fracture Mechanics, 2020, 224: 106814. DOI: 10.1016/j. engfracmech.2019.106814.

[43] SARKAR S, KUMAR R, MURTHY V M S R. Experimental and numerical simulation of crack propagation in sandstone by semi circular bend test [J]. Geotechnical and Geological Engineering, 2019, 37(4): 3157−3169. DOI: 10.1007/s10706-019-00833-0.

[44] BAŽANT Z P. Size effect on structural strength: A review [J]. Archive of Applied Mechanics, 1999, 69(9, 10): 703 – 725. DOI: 10.1007/s004190050252.

[45] PALANISWAMY K, KNAUSS W G. Propagation of a crack under general, in-plane tension [J]. International Journal of Fracture Mechanics, 1972, 8(1): 114 – 117. DOI: 10.1007/BF00185207.

[46] HUSSAIN M, PU L, UNDERWOOD J. Strain energy release rate for a crack under combined mode I and mode II. Fracture analysis [C]// Proceedings of the 1973 National Symposium on Fracture Mechanics: Part II. ASTM International,1974.

[47] UEDA Y, IKEDA K, YAO T, et al. Characteristics of brittle fracture under general combined modes [C]// Proceedings of ICF International Symposium on Fracture Mechanics. Beijing: Science Press, 1983.

[48] SIH G C. Strain-energy-density factor applied to mixed mode crack problems [J]. International Journal of Fracture, 1974, 10(3): 305−321. DOI: 10.1007/BF00035493.

[49] ERDOGAN F, SIH G C. On the crack extension in plates under plane loading and transverse shear [J]. Journal of Basic Engineering, 1963, 85(4): 519 – 525. DOI: 10.1115/1.3656897.

[50] KHAN S M A, KHRAISHEH M K. Analysis of mixed mode crack initiation angles under various loading conditions [J]. Engineering Fracture Mechanics, 2000, 67(5): 397 – 419. DOI: 10.1016/S0013-7944(00)00068-0.

[51] JANSSEN M, ZUIDEMA J, WANHILL R. Fracture Mechanics [M]. CRC Press, 2004. DOI: 10.1201/9781482265583.

[52] AYATOLLAHI M R, ALIHA M R M. On determination of mode II fracture toughness using semi-circular bend specimen [J]. International Journal of Solids and Structures, 2006, 43(17): 5217 – 5227. DOI: 10.1016/j. ijsolstr. 2005. 07.049.

[53] ALIHA M R M, AYATOLLAHI M R. Analysis of fracture initiation angle in some cracked ceramics using the generalized maximum tangential stress criterion [J]. International Journal of Solids and Structures, 2012, 49(13): 1877−1883. DOI: 10.1016/j.ijsolstr.2012.03.029.

[54] SMITH D J, AYATOLLAHI M R, PAVIER M J. The role of T-stress in brittle fracture for linear elastic materials under mixed-mode loading [J]. Fatigue & Fracture of Engineering Materials & Structures, 2001, 24(2): 137−150. DOI: 10.1046/j.1460-2695.2001.00377.x.

[55] SCHMIDT R A. A microcrack model and its significance to hydraulic fracturing and fracture toughness testing [C]// The 21st US Symposium on Rock Mechanics (USRMS). American Rock Mechanics Association, 1980.

[56] AYATOLLAHI M R, SISTANINIA M. Mode II fracture study of rocks using Brazilian disk specimens [J]. International Journal of Rock Mechanics and Mining Sciences, 2011, 48(5): 819 – 826. DOI: 10.1016/j.ijrmms. 2011.04.017.

[57] C L C, J W. On crack initiation angle of mixed mode ductile fracture with continuum damage mechanics [J]. Engineering

Fracture Mechanics, 1989, 32(4): 601－612. DOI: 10.1016/0013-7944(89)90194-X.

[58] HORII H, NEMAT-NASSER S. Compression-induced microcrack growth in brittle solids: Axial splitting and shear failure [J]. Journal of Geophysical Research: Solid Earth, 1985, 90(B4): 3105−3125. DOI: 10.1029/JB090iB04p03105.

[59] Brittle failure in compression: Splitting faulting and brittle-ductile transition [J]. Philosophical Transactions of the Royal Society of London Series A, Mathematical and Physical Sciences, 1986, 319(1549): 337−374.

(Edited by FANG Jing-hua)

中文导读

基于非对称半圆弯曲试件(ASCB)测定花岗岩的I/II断裂力学行为

摘要：非对称半圆弯曲试件(ASCB)以结构简单、加工经济、实验实施便利等优点广泛应用于建筑材料的断裂力学行为研究，然而，目前很少使用ASCB试件测定岩石的断裂特征。本文采用不同裂纹长度的花岗岩ASCB试样，研究花岗岩的断裂韧度值、裂纹开裂角以及裂纹扩展轨迹等断裂力学行为。首先，分析裂纹长度对纯I/II型断裂韧度的影响。然后，结合多种混合断裂理论，分析对比断裂韧度比值理论值与试验值的差异，以及断裂理论预测开裂角及实验测量值的差异，得到了预测混合断裂韧度及裂纹断裂角的最优准则。最后，探讨了半圆弯曲、非对称半圆弯曲试件测量岩石材料断裂力学特性时存在的不足之处。研究发现，当断裂过程区尺寸为2.6 mm时，采用广义最大环向拉应力准则能够很好地预测裂纹断裂角。在使用非对称半圆弯曲试件执行岩石断裂实验时，应把预制裂纹切割更深，即调整裂纹长度与试件半径的比值达到更大。本文的研究结果将为工程岩体断裂失稳机制的研究提供参考。

关键词：非对称半圆弯曲(ASCB)试件；断裂韧度；裂纹扩展轨迹；裂纹开裂角；半圆弯曲(SCB)；广义最大环向拉应力(GMTS)准则